

Properties of a diagonal two-orbital ladder model of the iron pnictide superconductors

E. Berg,^{1,2} S. A. Kivelson,² and D. J. Scalapino³

¹Department of Physics, Harvard University, Cambridge, Massachusetts 02138, USA

²Department of Physics, Stanford University, Stanford, California 94305-4045, USA

³Department of Physics, University of California, Santa Barbara, California 93106-9530, USA

(Received 11 March 2010; published 18 May 2010)

We study a diagonal two-orbital ladder model of the Fe-based superconductors using the density-matrix renormalization-group method. At half filling, we find a close competition between a “spin-stripped” state and a noncollinear “spin-checkerboard” state, as well as significant nematic correlations. Upon finite hole or electron doping, the dominant pairing correlations are found to have A_{1g} (S -wave) symmetry.

DOI: [10.1103/PhysRevB.81.172504](https://doi.org/10.1103/PhysRevB.81.172504)

PACS number(s): 74.70.Xa, 74.20.Mn, 71.27.+a, 74.20.Rp

I. INTRODUCTION

The recent discovery of iron pnictide superconductors¹ has added to the list of materials for which the superconducting pairing mechanism appears to be of electronic origin. From a theoretical point of view, these materials provide us with a rare opportunity to test our understanding of unconventional superconducting mechanisms. Numerous models have been proposed for these materials. In order for these models to be more tractable, most authors have taken either a weak-coupling^{2–8} or a strong-coupling^{9–12} starting point (i.e., assuming that the interaction strength is either much smaller or much larger than the bandwidth). However, there is evidence that the actual materials are in the *intermediate coupling* regime,^{13–17} which is also the most difficult to treat analytically. In this regime, one has to resort to numerical methods,^{15,16,18–20} which are currently limited to either small clusters or to one-dimensional systems. Despite these limitations, one may still hope that the important ordering tendencies of the system (which are presumably driven by short-range microscopic energetics) may be apparent already for small-size systems.

In this Brief Report, we study a two-orbital diagonal ladder model of the pnictides. The model is solved using the density-matrix renormalization-group (DMRG) (Ref. 21) technique, which enables us to study the sensitivity of the results to the system size in one direction. The diagonal geometry has the advantage that it preserves the symmetry between the x and y directions, thus enabling us to address some of the outstanding questions of the field, such as the question of the gap symmetry and of nematic ordering. For example, the reflection symmetry of the model makes the distinction between A_{1g} like (S wave) and B_{2g} like ($D_{x^2-y^2}$ wave) precise.

II. MODEL

The geometry of the model is shown in Fig. 1. Starting from the two-dimensional (2D) square Fe lattice, we cut out four parallel chains directed along $(1, -1)$. We then impose periodic boundary conditions in the transverse direction, such that Fe atoms separated by $\Delta\mathbf{R}=2a(1, 1)$ are identified. (a is the Fe-Fe spacing.) For each Fe site we keep one d_{xz} and one d_{yz} orbital. The Hamiltonian is written as $H=H_0+H_{\text{int}}$, where⁴

$$H_0 = \sum_{\mathbf{R}, \sigma} \left[-t_1 d_{x\sigma, \mathbf{R}}^\dagger d_{x\sigma, \mathbf{R}+a\hat{x}} - t_2 d_{x\sigma, \mathbf{R}}^\dagger d_{x\sigma, \mathbf{R}+a\hat{y}} + \sum_{\xi=\pm 1} (-t_3 d_{x\sigma, \mathbf{R}}^\dagger d_{x\sigma, \mathbf{R}+\eta} - \xi t_4 d_{x\sigma, \mathbf{R}}^\dagger d_{y\sigma, \mathbf{R}+\eta}) + \text{H.c.} - \mu n_{x, \mathbf{R}} + (x \leftrightarrow y) \right], \quad (1)$$

where $\eta=(a, \xi a)$, and

$$H_{\text{int}} = \sum_{\mathbf{R}} \left[\sum_{\alpha=x, y} U n_{\alpha\uparrow, \mathbf{R}} n_{\alpha\downarrow, \mathbf{R}} + V n_{x, \mathbf{R}} n_{y, \mathbf{R}} - J \mathbf{S}_{x, \mathbf{R}} \cdot \mathbf{S}_{y, \mathbf{R}} + J' (d_{x\uparrow, \mathbf{R}}^\dagger d_{x\downarrow, \mathbf{R}}^\dagger d_{y\downarrow, \mathbf{R}} d_{y\uparrow, \mathbf{R}} + \text{H.c.}) \right]. \quad (2)$$

Here, $d_{\alpha\sigma, \mathbf{R}}^\dagger$ with $\alpha=x, y$ creates an electron at site \mathbf{R} with spin σ in the d_{xz} and d_{yz} orbitals, respectively. We have defined $n_{\alpha\sigma}=d_{\alpha\sigma}^\dagger d_{\alpha\sigma}$, $n_\alpha=n_{\alpha\uparrow}+n_{\alpha\downarrow}$, and $\mathbf{S}_\alpha=\sum_{\sigma\sigma'} d_{\alpha\sigma}^\dagger \frac{\boldsymbol{\tau}_{\sigma\sigma'}}{2} d_{\alpha\sigma'}$, where $\boldsymbol{\tau}$ are Pauli matrices. In Eq. (1) we have used the tight-binding parameters which were obtained in Ref. 4: $t_1=-1$, $t_2=1.3$, $t_3=t_4=-0.85$. (We will henceforth measure all energies in units of $|t_1|$.) The interaction parameters in Eq. (2) were chosen to satisfy the constraints $U-V=\frac{5}{4}J$, $J'=J/2$ which follow from assuming a rotationally invariant Fe

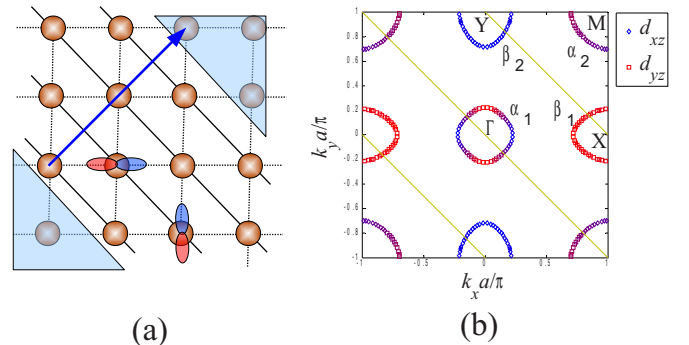


FIG. 1. (Color online) (a) The diagonal ladder geometry. Each site has two orbitals, d_{xz} and d_{yz} . Sites separated by $(2a, 2a)$ (indicated by the arrow in the figure) are identified. (b) The Brillouin zone of the two-band model (Ref. 4) in the unfolded (one Fe/unit cell) scheme. The Fermi surfaces are shown, along with their orbital content. The diagonal lines show the k states which can be accessed in the diagonal ladder.

atom. (To check the sensitivity of the results to parameters, we repeated the calculations using $U-V=J$. The results did not change qualitatively.) In order to reduce the number of parameters, we fixed $J=\frac{U}{4}$. Most of the calculations described below were done with $U=4-8$, which is in the “intermediate coupling” regime (such that U is smaller than the overall bandwidth, but larger than the Fermi energy of the electron and hole pockets).

In k space, the diagonal ladder geometry can be thought of as cutting through the 2D (one Fe/unit cell) Brillouin zone along the lines $\mathbf{k}=k_1(1,-1)+k_2(0,1)$, where $k_1 \in [-\frac{\pi}{a}, \frac{\pi}{a}]$ and $k_2=0$ or $\frac{\pi}{a}$. The resulting allowed points in k space are shown in Fig. 1(b), along with the Fermi surface of the two-band model at half filling (one electron per orbital). The two-orbital model has several well-known shortcomings: the α_2 pocket is centered at $(\frac{\pi}{a}, \frac{\pi}{a})$, while density-functional theory calculations show it at $(0,0)$, and the d_{xy} contribution which appears on parts of the Fermi surface is missing. However, as we will discuss, the important interplay between d_{xz} and d_{yz} is taken into account.

The diagonal ladder has translational symmetry and reflection symmetry with respect to two mirror planes which are formed by the z axis and a line in the $(1, \pm 1)$ directions that passes through a site. (Note that these reflection operations interchange d_{xz} and d_{yz} orbitals.) Therefore, the diagonal ladder can support a “nematic” phase in which the symmetry between x and y directions is spontaneously broken. In addition, there is a sharp symmetry distinction between an A_{1g} and a B_{1g} superconducting order parameter: A_{1g} is even under reflection through the mirror planes and B_{1g} is odd. A_{1g} and B_{2g} (D_{xy}) are not distinct, since they are both even under reflection. However, one can still distinguish between A_{1g} - and B_{2g} -like order parameters according to the relative sign of the order parameter on $(1,1)$ and $(1,-1)$ oriented bonds.

III. MAGNETIC AND NEMATIC CORRELATIONS

We begin from the half-filled case (one electron per orbital). In order to study the ordering tendencies of the system, we apply various types of symmetry-breaking perturbations at the edge and study how they propagate into the bulk.

In the DMRG calculations described below, we have kept up to $m=6000$ states in situations where both the number of particles and the z component of the total spin are conserved, and up to 3600 states in cases where one of these conservation laws is not present. The maximum truncation error was less than 4×10^{-4} in all cases.

Figure 2 shows the expectation value of the total magnetization $\mathbf{m}=\sum_a \langle \mathbf{S}_a \rangle$ as a function of position in a $4\sqrt{2}a \times \sqrt{2}a$ system with $U=8$. The total number of sites is 16 (32 orbitals). In these calculations, a Zeeman-field term of the form $-h_{\mathbf{R}} \cdot \mathbf{S}_{\mathbf{R}}$ was applied to two sites near the upper left edge, $\mathbf{R}=(0,0)$ and $(a,0)$. In Fig. 2(a), the fields were $\mathbf{h}_{(0,0)}=h\hat{z}$ and $\mathbf{h}_{(a,0)}=-h\hat{x}$, while in Fig. 2(b) the fields were $\mathbf{h}_{(0,0)}=\mathbf{h}_{(a,0)}=h\hat{z}$. The magnitude of the fields was $h=0.5$. As can be seen in the figure, these edge fields pin very different ordering patterns. The pattern in Fig. 2(b) is the “spin-striped” pattern with momentum $(0, \frac{\pi}{a})$, while in Fig. 2(a) we

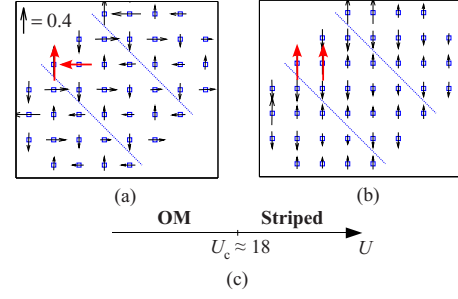


FIG. 2. (Color online) [(a) and (b)] Spin patterns in $4\sqrt{2}a \times \sqrt{2}a$ half-filled (two electrons per site) systems. The arrows are proportional to the local $\langle \mathbf{S} \rangle$. The diagonal dashed lines show the actual boundaries of the system. Zeeman fields of strength $h=0.5$ were applied on $(0,0)$ and $(1,0)$ sites, in the directions indicated by the bold arrows. (c) A schematic phase diagram at half filling.

find a “checkerboard” phase in which the magnetization on each of the two sublattices is orthogonal to the other, and both $(\frac{\pi}{a}, 0)$ and $(0, \frac{\pi}{a})$ momentum components are present. This phase has been found in unrestricted Hartree-Fock calculations,²² and has been termed “orthomagnetic” (OM). The ground-state energies in these two ordered states are equal within our numerical accuracy. In order to determine which of these states is the true ground state, we have undertaken two independent approaches. We have computed the ground-state energy of systems with $N=8-16$ sites, in the presence of a bulk ordering field of strength $h=0.5$ on each site with a pattern of orientations which forces the spin orders in Figs. 2(a) and 2(b). For $U \leq 18$, we have found for all system sizes studied that the energy of the OM pattern is lower than that of the striped pattern by a small amount of about 10^{-3} per site. Conversely, for larger U we find that the stripe pattern has a lower energy. We have obtained similar results from an analysis of the “spin-nematic” order, $\mathcal{N}_{\mathbf{R}} = \langle 3(S_{\mathbf{R}}^x)^2 - S_{\mathbf{R}}^2 \rangle$ measured on sites \mathbf{R} on one sublattice with a staggered Zeeman field, $-hS^z$ applied to the other sublattice; positive values of $\mathcal{N}_{\mathbf{R}}$ are indicative of stripe and negative values of OM ordering tendencies.

The fact that the OM and the striped states are nearly degenerate can be understood as a consequence of the magnetic frustration of the exchange interactions between the two sublattices.^{9,10,13} In the strong-coupling limit, $U \gg 1$, the two-band model maps onto a spin-1 Heisenberg model with a nearest-neighbor exchange interaction J_1 and a next-nearest neighbor J_2 . In the regime $J_2 > 0.5J_1$, the classical ($S \rightarrow \infty$) ground state consists of antiferromagnetically aligned A and B sublattices, while their relative orientation is completely free. However, $1/S$ quantum fluctuations favor the striped state over the OM state. This accounts for the weak preference for stripe order for $U \geq 18$. However, for somewhat smaller U , biquadratic spin-interaction terms of the form $K(\mathbf{R}_1, \dots, \mathbf{R}_4)(\mathbf{S}_{\mathbf{R}_1} \cdot \mathbf{S}_{\mathbf{R}_2})(\mathbf{S}_{\mathbf{R}_3} \cdot \mathbf{S}_{\mathbf{R}_4})$ are generated. Since their magnitude is of order $\frac{t^4}{U^3} \sim J^2/U$, they are negligible in the large- U limit, but (at least for the parameters we have explored) they produce a weak preference for the OM state for $U < 18$.

In the parent FeAs compounds, the ground state has a striped spin pattern, in contrast to our model in the realistic

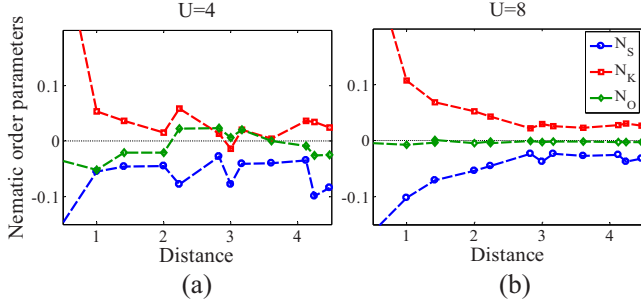


FIG. 3. (Color online) Measurements of the nematic order parameters [see Eq. (3)] as a function of distance from the origin, in $4\sqrt{2}a \times \sqrt{2}a$ (16 site) systems. (The geometry is the same as in the clusters shown in Fig. 2.) (a) $U=4$ and (b) $U=8$. In these calculations, the hopping strengths of the bond from $(0,0)$ to $(a,0)$ (at the upper left corner of the system) were 50% stronger than in the bulk.

intermediate-coupling regime. Since the OM and the striped states are extremely close in energy, it is easy to understand how small perturbations, e.g., slightly different model parameters or the coupling to the lattice, can stabilize the striped state relative to the OM state.

The striped state breaks the C_4 symmetry of the square 2D lattice down to C_2 , and thus this state has a “nematic” component. In the diagonal ladder geometry, the nematic character appears as a breaking of reflection symmetry about the $(1, \pm 1)$ directions. It is therefore interesting to calculate the nematic response of the system. We define the nematic order parameters

$$N_S(\mathbf{R}) = \sum_{\alpha} \langle [\mathbf{S}_{\alpha,\mathbf{R}} \cdot \mathbf{S}_{\alpha,\mathbf{R}+a\hat{x}} - \mathbf{S}_{\alpha,\mathbf{R}} \cdot \mathbf{S}_{\alpha,\mathbf{R}-a\hat{y}}] \rangle,$$

$$N_K(\mathbf{R}) = 2 \sum_{\alpha,\sigma} [|\langle d_{\alpha,\sigma,\mathbf{R}}^\dagger d_{\alpha,\sigma,\mathbf{R}+a\hat{x}} \rangle| - |\langle d_{\alpha,\sigma,\mathbf{R}}^\dagger d_{\alpha,\sigma,\mathbf{R}-a\hat{y}} \rangle|],$$

$$N_O(\mathbf{R}) = \langle [n_{x,\mathbf{R}} - n_{y,\mathbf{R}}] \rangle. \quad (3)$$

These order parameters were measured in a calculation in which the hopping strength on the bond from $(0,0)$ to $(a,0)$ was enhanced by 50% relative to the bulk, thus breaking reflection symmetry about $(1, -1)$ locally. Figure 3 shows the order parameters as a function of the distance from the boundary at which the perturbation is applied.

After an initial decay, N_S and N_K saturate and remain nearly constant. For $U=4$, there is some degree of “orbital order” N_O , which seems to fluctuate around zero. For $U=8$, N_O is very small, as can be expected from the fact that strong repulsive interactions suppress both intraorbital and interorbital density fluctuations. The substantial nematic correlations reflect the closeness in energy of the spin-striped state to the ground state.

IV. PAIRING CORRELATIONS

In order to study the pairing response of the system, we have added a boundary pairing potential of the form

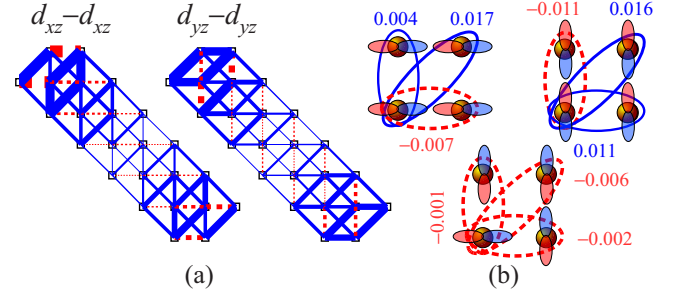


FIG. 4. (Color online) (a) Bond-pairing amplitudes for a $6\sqrt{2}a \times \sqrt{2}a$ (24 site) system with $U=4$, doped with six holes. Left: $d_{xz}-d_{xz}$ pairing and right: $d_{yz}-d_{yz}$ pairing. An external pairing field of strength $\Delta=0.5$ is applied to the upper left diagonal $d_{xy}-d_{xy}$ bond [see Eq. (4)], highlighted in the figure. The thickness of the bonds represents the amplitude of induced pair field on that bond. Solid (dashed) lines stand for positive (negative) amplitudes, respectively. (b) Detailed pair structure near the middle of the system. Upper left: $d_{xz}-d_{xz}$ amplitudes, upper right: $d_{yz}-d_{yz}$, and bottom: $d_{xz}-d_{yz}$ amplitudes.

$$H_1 = -\Delta [d_{x,\uparrow,\mathbf{R}_1}^\dagger d_{x,\downarrow,\mathbf{R}_2}^\dagger - d_{x,\downarrow,\mathbf{R}_1}^\dagger d_{x,\uparrow,\mathbf{R}_2}^\dagger + \text{H.c.}], \quad (4)$$

where $\mathbf{R}_1=(0,0)$ and $\mathbf{R}_2=(a,a)$. This term can be thought of as a proximity coupling to a bulk superconductor. Note that since the pairing term is applied only to the d_{xz} orbital, it couples to any (singlet) superconducting order parameter.

Figure 4(a) shows the induced bond pair amplitudes $\phi_{\mathbf{R},\mathbf{R}'} = \langle d_{\alpha,\uparrow,\mathbf{R}}^\dagger d_{\alpha,\downarrow,\mathbf{R}'}^\dagger - d_{\alpha,\downarrow,\mathbf{R}}^\dagger d_{\alpha,\uparrow,\mathbf{R}'}^\dagger + \text{H.c.} \rangle$ for a $6\sqrt{2}a \times \sqrt{2}a$ (24 site) system with $\Delta=0.5$ and $U=4$. With the pair field term in Eq. (4), the number of electrons in the system is not conserved. Here, we choose the chemical potential μ such that the average number of electrons in the system is close to 42, which corresponds to a hole doping of $n=0.25$ per Fe site. The pair amplitudes decay slowly with the distance from the edge. Near the middle of the system, the pair structure is shown in Fig. 4(b). One can see that under reflection about the $(1, \pm 1)$ directions, the pair wave function is *even*, indicating A_{1g} -like pairing. The A_{1g} structure appears already in smaller systems (down to $2\sqrt{2}a \times \sqrt{2}a$). The same pairing occurs in electron-doped systems and even in the undoped system, although here the pairing response is considerably weaker. For $U=8$, the pairing symmetry is still A_{1g} , although the pairing amplitude decays considerably faster than for $U=4$.

Figure 5 shows the diagonal $d_{xz}-d_{xz}$ and $d_{yz}-d_{yz}$ pairing amplitude as a function of position, in calculations with various pairing potentials applied at the edge, such that they excite different pairing symmetries selectively. For A_{1g} , Eq. (4) was used. For B_{1g} , we have added an additional term for the d_{yz} orbital, with an opposite sign. This term does not couple to the A_{1g} pairing symmetry at all, because it is odd under reflection about $(1, -1)$. In addition, we have applied a triplet pairing term [in which the sign in the square brackets of Eq. (4) is reversed]. Strictly speaking, the B_{2g} (D_{xy} -like) symmetry is not distinct from A_{1g} . However, one can still think about a “ B_{2g} -like” pair structure in which the sign of the pair amplitude on $(1,1)$ - and $(1,-1)$ -oriented bonds is

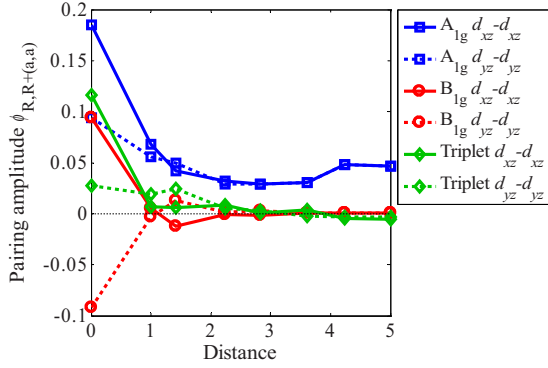


FIG. 5. (Color online) Induced pair amplitudes on diagonal bonds in three $4\sqrt{2}a \times \sqrt{2}a$ calculations, in which A_{1g} (\square), B_{1g} (\circ), and triplet (\diamond) pair fields are applied to the edge (see text). Solid (dashed) lines correspond to d_{xz} - d_{xz} (d_{yz} - d_{yz}) pairing, respectively.

opposite. To couple mostly to B_{2g} , we have added to Eq. (4) a bond-pairing term on the $(0,0)$ - $(a,-a)$ bond with an equal magnitude and opposite sign. Alternatively, we have applied a singlet d_{xz} - d_{yz} pair field on the $(0,0)$ - $(a,0)$ bond, which also favors B_{2g} -like pairing. Comparing the response of the different pairing symmetries, the A_{1g} pairing clearly decays much more slowly than the triplet and the B_{1g} pairings. In the B_{2g} calculations (not shown), the induced pairing structure is B_{2g} like very close to the edge, but changes its character to A_{1g} like further away into the bulk.

V. DISCUSSION

In conclusion, the two-orbital diagonal ladder model shows several robust features, which appear already at very small system sizes. In electron- and hole-doped systems, there is a clear tendency to form A_{1g} (S -wave) superconduct-

ing order. All other forms of order are very weak. For the undoped system, a strong tendency toward antiferromagnetic ordering is observed. However, two forms of magnetic order are in close competition with each other: unidirectional “stripe” order, of the sort found in experiment, and noncolinear “spin-checkerboard” (OM) order, which was found also in mean-field calculations.²² In our model, the spin-stripped state is stabilized for $U \geq 18$ and the OM is stabilized for smaller values of U . The near degeneracy of these two states implies that small terms can tilt the balance one way or the other, which raises the possibility that the OM state may be stabilized in some member of the Fe pnictide or chalcogen families. Finally, in the undoped system there is a strong tendency toward nematic order. This order is associated with the expectation values of bond operators (e.g., the local kinetic energy and spin-spin correlations), rather than the difference of on-site orbital occupations which were found to be small.

ACKNOWLEDGMENTS

We are grateful to E. Dagotto, J. Lorenzana, A. Moreo, F. Pollmann, and W.-F. Tsai for their comments on this manuscript. D.J.S. acknowledges the Center for Nanophase Materials Science at ORNL, which is sponsored by the Division of Scientific User Facilities, U.S. DOE, and thanks SITP at Stanford for their hospitality. S.A.K. was supported, in part, by the NSF under Grant No. DMR-0758356. E.B. was supported by the NSF under Grants No. DMR-0705472 and No. DMR-0757145. We acknowledge the Center for Nanoscale Systems (CNS) (supported by NSF under Award No. ECS-0335765) at Harvard University, for allocation of computer time through the Odyssey cluster supported by the FAS Research Computing Group. This work was supported, in part, by the NSF under Grant No. PHY05-51164 at the KITP.

- ¹Y. Kamihara, T. Watanabe, M. Hirano, and H. Hosono, *J. Am. Chem. Soc.* **130**, 3296 (2008).
- ²I. I. Mazin, D. J. Singh, M. D. Johannes, and M. H. Du, *Phys. Rev. Lett.* **101**, 057003 (2008).
- ³K. Kuroki, S. Onari, R. Arita, H. Usui, Y. Tanaka, H. Kontani, and H. Aoki, *Phys. Rev. Lett.* **101**, 087004 (2008).
- ⁴S. Raghu, X. L. Qi, C. X. Liu, D. J. Scalapino, and S. C. Zhang, *Phys. Rev. B* **77**, 220503(R) (2008).
- ⁵F. Wang, H. Zhai, Y. Ran, A. Vishwanath, and D. H. Lee, *Phys. Rev. Lett.* **102**, 047005 (2009).
- ⁶A. V. Chubukov, D. V. Efremov, and I. Eremin, *Phys. Rev. B* **78**, 134512 (2008).
- ⁷S. Graser, T. A. Maier, P. J. Hirschfeld, and D. J. Scalapino, *New J. Phys.* **11**, 025016 (2009).
- ⁸V. Cvetkovic and Z. Tešanović, *Europhys. Lett.* **85**, 37002 (2009); *Phys. Rev. B* **80**, 024512 (2009).
- ⁹C. Fang, H. Yao, W. F. Tsai, J. P. Hu, and S. A. Kivelson, *Phys. Rev. B* **77**, 224509 (2008).
- ¹⁰C. Xu, Y. Qi, and S. Sachdev, *Phys. Rev. B* **78**, 134507 (2008).
- ¹¹K. Seo, B. A. Bernevig, and J.-P. Hu, *Phys. Rev. Lett.* **101**, 206404 (2008).

- ¹²F. Krüger, S. Kumar, J. Zaanen, and J. van den Brink, *Phys. Rev. B* **79**, 054504 (2009).
- ¹³Q. Si and E. Abrahams, *Phys. Rev. Lett.* **101**, 076401 (2008).
- ¹⁴Q. Si, E. Abrahams, J. Dai, and J.-X. Zhu, *New J. Phys.* **11**, 045001 (2009).
- ¹⁵K. Haule, J. H. Shim, and G. Kotliar, *Phys. Rev. Lett.* **100**, 226402 (2008).
- ¹⁶M. Aichhorn, L. Pourovskii, V. Vildosola, M. Ferrero, O. Parcollet, T. Miyake, A. Georges, and S. Biermann, *Phys. Rev. B* **80**, 085101 (2009).
- ¹⁷M. M. Qazilbash, J. J. Hamlin, R. E. Baumbach, L. Zhang, D. J. Singh, M. B. Maple, and D. N. Basov, *Nat. Phys.* **5**, 647 (2009).
- ¹⁸M. Daghofer, A. Moreo, J. A. Riera, E. Arrigoni, D. J. Scalapino, and E. Dagotto, *Phys. Rev. Lett.* **101**, 237004 (2008).
- ¹⁹A. Moreo, M. Daghofer, J. A. Riera, and E. Dagotto, *Phys. Rev. B* **79**, 134502 (2009).
- ²⁰E. Berg, S. Kivelson, and D. Scalapino, *New J. Phys.* **11**, 085007 (2009).
- ²¹S. R. White, *Phys. Rev. Lett.* **69**, 2863 (1992).
- ²²J. Lorenzana, G. Seibold, C. Ortix, and M. Grilli, *Phys. Rev. Lett.* **101**, 186402 (2008).